PHYSICAL REVIEW A **81**, 051603(R) (2010)

Probing the Kondo lattice model with alkaline-earth-metal atoms

Michael Foss-Feig,[1,2] Michael Hermele,[1] and Ana Maria Rey[1,2,3]
[1]*Department of Physics, University of Colorado, Boulder, Colorado 80309, USA*
[2]*JILA, Boulder, Colorado 80309, USA*
[3]*NIST, Boulder, Colorado 80309, USA*
(Received 11 January 2010; published 7 May 2010)

We study transport properties of alkaline-earth-metal atoms governed by the Kondo lattice Hamiltonian plus a harmonic confining potential, and suggest simple dynamical probes of several different regimes of the phase diagram that can be implemented with current experimental techniques. In particular, we show how Kondo physics at strong coupling, at low density, and in the heavy fermion phase is manifest in the dipole oscillations of the conduction band upon displacement of the trap center.

DOI: 10.1103/PhysRevA.81.051603 PACS number(s): 67.85.−d, 03.75.Ss, 37.10.Jk, 71.27.+a

To date, most cold atom simulations of condensed-matter systems have focused on the single-band Bose and Fermi Hubbard models, both because they are relatively simple to simulate and because they are believed to capture a great deal of important physics. However, there are many real materials in which the relevance of both internal (spin) and external (orbital) electronic degrees of freedom preclude description by the single-band Hubbard model. Recently it has been shown that fermionic alkaline-earth-metal atoms (AEMAs) have unique properties that allow for the simulation of Hamiltonians with both spin and orbital degrees of freedom [1], without recourse to superlattice structures [2] or population of excited bands [3]. There has also been substantial recent progress in cooling these atoms to quantum degeneracy [4–8]. Here we discuss avenues thereby opened into optical lattice simulations of the Kondo lattice model (KLM).

As is generally the case, the necessity to perform a cold atom simulation in a trap complicates the analogy with the translationally invariant KLM. However, in this Rapid Communication we emphasize how a trap can help reveal hallmarks of the KLM, including heavy fermion mass enhancement (through dynamics induced by trap displacement) and the Kondo insulator gap (through formation of a density plateau). The proposed experimental probing methods (center-of-mass oscillations [9–11] and shell-structure density profiles [12,13]) have been demonstrated to be successful diagnostic tools in alkali-metal atoms and, therefore, we expect that our analysis will have direct applicability in experiments done in the near future with AEMAs.

In its standard form, the KLM consists of a band of conduction electrons interacting via a contact Heisenberg exchange with a lattice of immobile spins. We focus on the case of antiferromagnetic (AF) exchange, relevant to so-called heavy fermion materials, which are known for radically enhanced quasiparticle masses [14]. Simulation of the KLM Hamiltonian with AEMAs was described in [1]; here we only summarize the basic idea.

The $^1S_0$ (g) and $^3P_0$ (e) clock states of an AEMA can be trapped independently in two different optical lattice potentials whose periodicities could be engineered to be the same [15]. We can therefore consider a Mott insulator of e atoms (immobile spins) trapped in the vibrational ground state of a deep optical lattice that coexists with mobile g atoms (conduction electrons) trapped in the vibrational ground state of a shallow lattice with the same periodicity. At low temperatures the interactions are determined by four s-wave scattering lengths a_{ee}, a_{gg}, and $a_{eg}^{\pm}$ for the states $|ee\rangle$, $|gg\rangle$, and $\frac{1}{\sqrt{2}}(|eg\rangle \pm |ge\rangle)$, respectively. We choose the e atoms to be localized because they would otherwise suffer lossy collisions. Collisions between g and e atoms, on the other hand, are expected to be mostly elastic [1]. The independence of the scattering lengths on the nuclear spin state guarantees that there will not be spin-changing collisions, and so we are justified in considering an ensemble with only two nuclear spin states $\sigma = \pm$ (the electron spin in the KLM).

If the g atoms have negligible interactions with each other (which is true to a very good approximation in ^{171}Yb) and the strong repulsion between e atoms is taken into account by a unit-filling constraint, the low-energy Hamiltonian contains only two interaction parameters $U_{eg}^{\pm} \propto a_{eg}^{\pm} \int d^3r\, w_e^2(r) w_g^2(r)$ (where w_α is the lowest Wannier orbital for the lattice containing the α atoms). By defining $V_{\mathrm{ex}} = (U_{eg}^{+} - U_{eg}^{-})/2$, dropping constant terms, and including a harmonic trap of curvature Ω, the Hamiltonian reduces to [1]

$$\mathcal{H}_K = -J_g \sum_{\langle i,j\rangle,\sigma} c_{ig\sigma}^{\dagger} c_{jg\sigma} + V_{\mathrm{ex}} \sum_{i\sigma\sigma'} c_{ig\sigma}^{\dagger} c_{ie\sigma'}^{\dagger} c_{ig\sigma'} c_{ie\sigma} + \Omega \sum_i i^2 n_{ig}. \quad (1)$$

Here $c_{i\alpha\sigma}^{\dagger}$ creates an atom at site i in the electronic state $\alpha \in \{e,g\}$ and (nuclear) spin state σ, $n_{i\alpha} \equiv \sum_\sigma c_{i\alpha\sigma}^{\dagger} c_{i\alpha\sigma}$, and J_g is the tunneling energy for the g atoms. The dimensionless ratios $v = -2V_{\mathrm{ex}}/J_g$ and $q = 4J_g/\Omega$, together with the number of g atoms N_g, characterize the various parameter regimes of the model. Unlike in previous proposals [2,3], here the parameters U_{ee}, U_{gg}, and v are mutually independent, and the entire KLM phase diagram is in principle accessible. For instance, both the sign and magnitude of V_{ex} will depend on the atomic isotope used, and the magnitude can be further adjusted by offsetting one lattice from the other (to decrease the overlap between Wannier orbitals) [1]. Therefore, in principle both ferromagnetic (FM) and AF exchange are relevant. Nevertheless, in this paper we exclusively consider the AF case ($v > 0$).

In this regime the phase diagram of the translationally invariant KLM in one dimension (Fig. 1) has been relatively

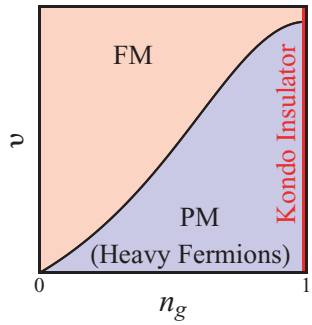

FIG. 1. (Color online) Schematic zero temperature phase diagram for the 1D KLM [16]. FM is a ferromagnetic phase, and PM is a paramagnetic phase closely related to heavy fermions in higher dimensions.

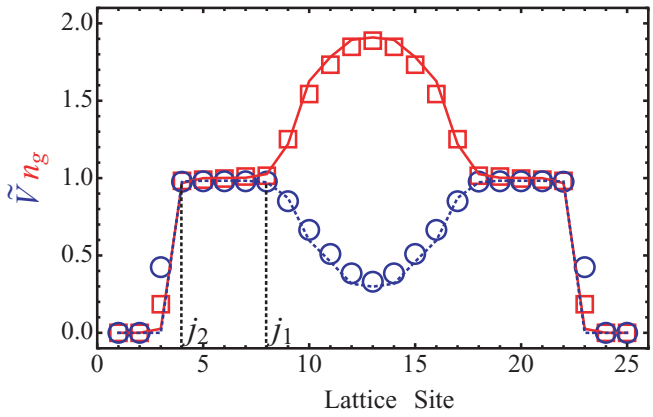

FIG. 2. (Color online) The hybridization gap Δ_H induces a plateau in the g atom density distribution (n_g, red solid line) and the hybridization ($\tilde{V}$, blue dotted line). Lines are from self-consistent MFT and open shapes from LDA. The parameters used for this plot were $N_g = 25$, $q = 40$, $v = 8$.

well established, and can be drawn consistently from a variety of numerical studies and several exact results [16]. At strong coupling ferromagnetism prevails, but the weak-coupling limit is paramagnetic (PM). The boundary $n_g = 1$ is insulating, having spin and charge gaps for arbitrarily small nonzero coupling. To our knowledge, the one-dimensional (1D) model is not realized in condensed-matter systems, but it could be explored with AEMAs in a three-dimensional (3D) optical lattice if both the e and g lattices were made deep in two of the dimensions (an array of 1D tubes).

Heavy fermions. We begin our analysis in the PM phase, which is closely related to heavy fermion behavior in higher dimensions [16]. The mass enhancement can be understood qualitatively through a hybridization mean-field decoupling [17] in which the quasiparticles near the Fermi surface have a strongly localized character. While the mean-field theory (MFT) does not capture the Luttinger liquid nature of the PM phase at low energies, we believe it nonetheless provides a reasonable guide to the phenomena discussed here; effects beyond MFT are left for future study. Moreover, in work to be presented elsewhere, the calculations to follow have been extended to a two-dimensional geometry where MFT is more reliable, with no qualitative change to the results.

The MFT can be obtained by a (nonunique) decoupling of the interaction term in $\mathcal{H}_K$, leading to

$$\mathcal{H}_{\mathrm{MFT}} = -J_g \sum_{\langle i,j\rangle\sigma} c^\dagger_{ig\sigma} c_{jg\sigma} + \sum_{i\sigma} [\Omega i^2 n_{ig} + \mu_i (n_{ie} - 1)] + V_{\mathrm{ex}} \sum_{i\sigma} \tilde{V}_i (c^\dagger_{ig\sigma} c_{ie\sigma} + \mathrm{H.c.}) - V_{\mathrm{ex}} \sum_i \tilde{V}_i^2. \quad (2)$$

In Eq. (2) we have defined $\tilde{V}_i = \frac{1}{2}\sum_\sigma \langle c^\dagger_{ie\sigma} c_{ig\sigma} + \mathrm{H.c.}\rangle$, where the expectation value is taken in the Slater determinant of the $(N_e + N_g)/2$ lowest-energy single-particle states (and the $1/2$ accounts for spin degeneracy). We have also introduced chemical potentials μ_i to enforce the local constraints $\langle n_{ie}\rangle = 1$. This decoupling is paramagnetic and therefore cannot capture any magnetism, but it does describe the tendency toward singlet formation at strong coupling. In addition, it turns out to be the exact $N \to \infty$ solution of the SU(N) generalization of the KLM [which can be implemented with AEMAs having nuclear spin $I = (N-1)/2$] [18,19]. Because $\mathcal{H}_{\mathrm{MFT}}$ is quadratic it can be diagonalized, but it is necessary to choose the $\tilde{V}_i$ self-consistently.

In the translationally invariant problem it is customary to assume $\tilde{V}_i = \tilde{V}$ and $\mu_i = \mu$, in which case analytic progress is possible. With the trap we retain the site-dependent $\tilde{V}_i$ and μ_i, and self-consistent solutions must be obtained numerically. The procedure involves an initial guess for the $\tilde{V}_i$ based on the local-density approximation (LDA): We treat the trap as a site-dependent chemical potential and infer the energy on each site from a translationally invariant problem. LDA results are obtained by minimization of the energy thus obtained, while obeying a constraint on the total particle number. We then solve for the μ_i that satisfy the local constraints [20], diagonalize $\mathcal{H}_{\mathrm{MFT}}$, and recalculate the $\tilde{V}_i$ using the definition. By iterating this procedure we arrive at a self-consistent solution.

From the MFT ground states we can easily compute the $\langle n_{ig}\rangle$, which give us density profiles in the trap. For N_g or Ω sufficiently large, these show plateaus (Fig. 2) similar to what is observed for the repulsive Hubbard model, although here they reflect the gap of a Kondo insulator, not a Mott insulator. The Kondo insulator is often understood within the MFT: Unit filling of g atoms corresponds to completely filling a hybridized band, and there is a charge gap of Δ_H. LDA considerations then imply that $\Omega(j_2^2 - j_1^2) = \Delta_H$ (Fig. 2). Exact results for the $v = \infty$ KLM give $\Omega(j_2^2 - j_1^2) = 3|V_{\mathrm{ex}}|$; in this limit Δ_H tends to $2|V_{\mathrm{ex}}|$, so the MFT underestimates the plateau size. For the bosonic Hubbard model, where the relevant gap is the on-site interaction U, such plateau structures have already been imaged via microwave spectroscopy [12,13]. We therefore expect that for large v the plateau can be observable experimentally.

At lower fillings, where the plateau does not form, we are everywhere in the heavy fermion metallic state. Under these conditions we consider an experiment where the trap center is suddenly displaced, causing dipole oscillations of the g atom center of mass (COM). This type of experiment has been implemented in alkali-metal atoms to study 1D and 3D transport of interacting bosons and fermions [9–11], and used to probe different quantum many-body regimes in these systems. We calculate these dynamics self-consistently, starting with the MFT ground states and shifting the Hamiltonian.

If $\alpha^\dagger_{q\sigma} = \sum_j (u^q_j c^\dagger_{jg\sigma} + v^q_j c^\dagger_{je\sigma})$ create the eigenstates of $\mathcal{H}_{\rm MFT}$, then the following set of discrete Schrödinger equations governs the evolution of the $u^q_j(t)$ and $v^q_j(t)$ after displacing the trap by δ lattice sites:

$$\begin{aligned} -i\dot{u}^q_j &= J_g\left(u^q_{j-1} + u^q_{j+1}\right) - \Omega\,(j-\delta)^2\,u^q_j - V_{\rm ex}\tilde{V}_j v^q_j, \\ -i\dot{v}^q_j &= -\Omega\,(j-\delta)^2\,v^q_j - \mu_j v^q_j - V_{\rm ex}\tilde{V}_j u^q_j. \end{aligned} \tag{3}$$

These are simply the Heisenberg equations of motion for the quasiparticles $d\alpha^\dagger_{q\sigma}/dt = i[\mathcal{H}^\delta_{\rm MFT}, \alpha^\dagger_{q\sigma}]$ (where $\mathcal{H}^\delta_{\rm MFT}$ is the translation of $\mathcal{H}_{\rm MFT}$ by δ lattice sites). When integrating these equations the $\tilde{V}_j$ are updated self-consistently and the μ_j are evolved in time by ensuring that $d^2\langle n_{je}\rangle/dt^2 = 0$ (the first time derivative has no dependence on the μ_j). Such time dependence of the μ_j preserves the one e atom per site constraint, and its necessity has a simple origin: $\mathcal{H}_{\rm MFT}$ breaks the local U(1) symmetry of $\mathcal{H}_K$ associated with conservation of the e atom density.

The g atom COM oscillations ensuing from displacement of the trap by one lattice site have been obtained at several values of v for fixed q. We find a strong enhancement of the oscillation period τ (and hence of the quasiparticle mass $m \sim \tau^2$) for decreasing $|V_{\rm ex}|$ (Fig. 3). Once $v \sim 1$, the comparably fast noninteracting oscillations emerge on top of the slow oscillations of the heavy quasiparticles, converging to the noninteracting result as $v \to 0$ (which cuts off the apparent trend toward diverging τ in Fig. 3).

Strong coupling. We now turn to the FM part of the phase diagram, which exists for all fillings at sufficiently strong coupling. When $v = \infty$ the ground state is formed by pairing each g atom into a spin singlet with one e atom. To first order in J_g the singlets become mobile, and there is an exact mapping of the unpaired e atoms to the fermions of a $U = \infty$ Hubbard model (with the singlets being the holes) [21]. Because nearest-neighbor hopping cannot exchange up and down spins, we can think of the fermions as spinless [22], perform a particle hole

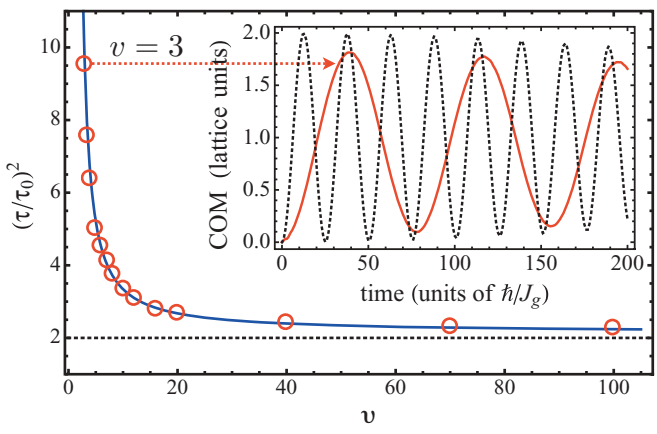

FIG. 3. (Color online) Enhancement of the g atom COM oscillation period (τ/τ_0) reveals the mass enhancement $(m/m_0 \sim \tau^2/\tau_0^2$, with m_0 and τ_0 the values at $v = 0$). The red circles are from MFT dynamics, the blue solid curve is a guide to the eye, and the black dotted line at $(\tau/\tau_0)^2 = 2$ marks the doubled effective mass expected from Eq. (4) at strong coupling. Inset: COM motion for $v = 3$ (red solid line) and $v = 0$ (black dotted line). In all cases the parameters used were $N_g = 5$ and $q \approx 235$.

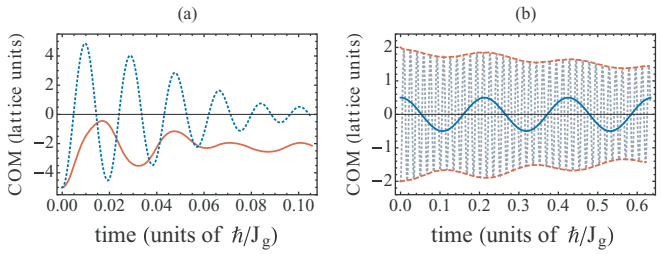

FIG. 4. (Color online) (a) The dotted blue line shows the noninteracting dynamics of 16 g atoms after displacement of the trap by five lattice sites. The solid red line shows the same dynamics except now with $v = \infty$ (calculated using $\mathcal{H}_\infty$). In both cases $q = 400$. (b) The polaron COM (gray dotted line) is shown oscillating after trap displacement by two lattice sites. The parameters used here were $q = 800$ and $v = 2$. For comparison we plot $\cos(V_{\rm ex}t)$ (blue solid line), showing that the energy gap determines the time scale of amplitude modulation (red dashed line). The overall decay is a finite-size effect and eventually revives.

transformation (now the singlets are spinless fermions), and thereby arrive at a simple Hamiltonian that describes the g atoms,

$$\mathcal{H}_\infty = -\frac{J_g}{2}\sum_{\langle i,j\rangle} c^\dagger_{ig}c_{jg} + \Omega\sum_i i^2 n_{ig}. \tag{4}$$

The reduction of the hopping energy is the result of projecting out the high-energy triplet states. To highlight this strong-coupling behavior, we again consider dynamics ensuing from a sudden displacement of the trap center. If the system is strongly interacting, Eq. (4) avails a simple treatment of these dynamics based on the noninteracting solutions in Ref. [23]. There the authors found that for $q \gg 1$ and $N_g \lesssim 4\sqrt{2J_g/\Omega}$ the dynamics involved *delocalized*, free-space harmonic-oscillator-like states with level spacing $\omega^* = \Omega\sqrt{q}$. At $v = \infty$ we effectively have $N_g \to 2N_g$ (because the fermions become spinless) and $J_g \to J_g/2$. Therefore, the inequality can be violated at strong coupling even when satisfied for the noninteracting system; *localized* states become populated and transport is strongly inhibited [Fig. 4(a)].

Weak coupling. Another limit which is well understood in the FM phase of the translationally invariant model is $N_g = 1$. Sigrist *et al.* [24] proved that the ground state of the KLM with L sites and one conduction electron has total spin $S = \frac{1}{2}(L-1)$, even in the absence of translational symmetry, and they described the excitations for the homogenous case as bound states between the g atom and a flipped spin in the deep lattice (spin polaron). For a weak trap ($q \gg 1$) and at sufficiently small coupling ($|V_{\rm ex}| \ll \omega^*$), we characterize the polaron spectrum to lowest order in degenerate perturbation theory and find that one eigenvalue separates from the rest by a gap of approximately $|V_{\rm ex}|$. As we see in Fig. 4(b), this energy scale manifests itself in the COM oscillations of a single g atom as a strong modulation of the oscillation amplitude with periodicity $\tau \approx \frac{2\pi}{|V_{\rm ex}|}$. This is verified by the dynamics calculated from the exact eigenstates of $\mathcal{H}_K$.

For the finite system under consideration, we expect this behavior will persist for $N_g > 1$ whenever N_g is odd. This can be understood by noting that a single unpaired g atom at the Fermi level gains energy at first order in perturbation theory when coupling to the e atoms is turned on, whereas the

doubly occupied levels below it do so only at second order. It is also worth noting that the condition $V_{ex} \ll \omega^*$ is equivalent to demanding the perturbation stay smaller than the finite-size gap. For fixed lattice depth and peak g atom density, the gap scaling is $\omega^* \sim 1/R$, with R the Thomas-Fermi radius of the g atom cloud ($R \propto \sqrt{N_g J_g/\omega^*}$). This means that the demonstrated modulations will be washed out with increasing $|V_{ex}|$ or with increasing g atom number and are thus manifestly a finite-size effect.

Experimental realization. We now consider the feasibility of generating and observing these dynamics in an experiment. Throughout this Rapid Communication we have assumed a unit-filled Mott insulator of e atoms coexisting with various fillings of g atoms at the center of a trap. To realize this situation in experiment, one could first ramp up a deep optical lattice for the g atoms so that they exhibit a Mott insulator shell structure. By taking advantage of the energy shift between double and single occupied sites, it is then possible to selectively transfer atoms into the e state so that sites with two gg atoms become eg sites and single occupied g sites become single occupied e sites. A subsequent adiabatic reduction of the lattice depth for the g atoms achieves the desired configuration. It may also be helpful to confine the g atoms more tightly than the e atoms (to ensure that they do not sample the wings of the e atom Mott insulator), which can be achieved by blue detuning the deep lattice. In most of our calculations we have used small trap displacements to simplify the numerics, and in a real experiment they will inevitably be larger. Observation of the dipole oscillations in 1D with an amplitude of $\lesssim 8$ lattice sites has precedent and was carried out by mapping the center-of-mass position of the atomic cloud to momentum space [9,10]. Moreover, a recent proposal [25] suggests that dynamics could be characterized from a single nondestructive measurement if the atoms are coupled to an unpumped cavity field. The small atom numbers necessary for observation of the modulations at small $|V_{ex}|$ also has precedent, with ~ 18 atoms per tube having been realized in an array of 1D lattices [26]. We emphasize that all physics discussed here involves energy scales on the order of V_{ex}, which makes temperature demands less constraining than for proposals involving superexchange or Ruderman-Kittel-Kasuya-Yosida-type physics. ($v \approx 1$ gives a Kondo temperature on the order of $|V_{ex}|/k_B$, so this statement applies even to the heavy fermion behavior.)

The results presented demonstrate that dipole oscillations of the g atom COM effectively probe a variety of KLM phenomena. The emphasis has been on a 1D system, which is of relevance to cold atom experiments, primarily because current theoretical understanding of the phase diagram is strongest here. However, the heavy fermion behavior generalizes to experiments in two and three dimensions. Although it has not been discussed, we point out that an optical lattice experiment (especially in $D > 1$) is a natural setting for probing the size of the Fermi surface in the heavy fermion state and could corroborate evidence for a large Fermi surface observed in condensed-matter experiments.

We thank Thomas Gasenzer, Matthias Kronenwett, Alexey Gorshkov, Maria Luisa Chiofalo, Brandon Peden, Victor Gurarie, and Jun Ye for helpful discussions. This work was supported by grants from the NSF (PFC and PIF-0904017), the DOE (DE-SC0003910), and a grant from the ARO with funding from the DARPA-OLE.

[1] A. V. Gorshkov *et al.*, Nature Phys. **6**, 289 (2010).
[2] B. Paredes, C. Tejedor, and J. I. Cirac, Phys. Rev. A **71**, 063608 (2005).
[3] L. M. Duan, Europhys. Lett. **67**, 721 (2004).
[4] T. Fukuhara, Y. Takasu, M. Kumakura, and Y. Takahashi, Phys. Rev. Lett. **98**, 030401 (2007).
[5] T. Fukuhara, S. Sugawa, and Y. Takahashi, Phys. Rev. A **76**, 051604(R) (2007).
[6] S. Stellmer, M. K. Tey, B. Huang, R. Grimm, and F. Schreck, Phys. Rev. Lett. **103**, 200401 (2009).
[7] S. Kraft, F. Vogt, O. Appel, F. Riehle, and U. Sterr, Phys. Rev. Lett. **103**, 130401 (2009).
[8] Y. N. Martinez de Escobar, P. G. Mickelson, M. Yan, B. J. DeSalvo, S. B. Nagel, and T. C. Killian, Phys. Rev. Lett. **103**, 200402 (2009).
[9] C. D. Fertig *et al.*, Phys. Rev. Lett. **94**, 120403 (2005).
[10] N. Strohmaier *et al.*, Phys. Rev. Lett. **99**, 220601 (2007).
[11] D. McKay, M. White, M. Pasienski, and B. DeMarco, Nature (London) **453**, 76 (2008).
[12] G. Campbell, J. Mun, M. Boyd, and P. Medley, Science **313**, 649 (2006).
[13] S. Fölling, A. Widera, T. Muller, F. Gerbier, and I. Bloch, Phys. Rev. Lett. **97**, 060403 (2006).
[14] S. Doniach, Physica B **91**, 231 (1977).
[15] A. J. Daley, M. M. Boyd, J. Ye, and P. Zoller, Phys. Rev. Lett. **101**, 170504 (2008).
[16] H. Tsunetsugu, M. Sigrist, and K. Ueda, Rev. Mod. Phys. **69**(3), 809 (1997).
[17] C. Lacroix and M. Cyrot, Phys. Rev. B **20**, 1969 (1979).
[18] P. Coleman, Phys. Rev. B **28**, 5255 (1983).
[19] N. Read, D. M. Newns, and S. Doniach, Phys. Rev. B **30**, 3841 (1984).
[20] M. Hermele, V. Gurarie, and A. M. Rey, Phys. Rev. Lett. **103**, 135301 (2009).
[21] C. Lacroix, Solid State Commun. **54**, 991 (1985).
[22] M. Ogata and H. Shiba, Phys. Rev. B **41**, 2326 (1990).
[23] A. M. Rey, G. Pupillo, C. W. Clark, and C. J. Williams, Phys. Rev. A **72**, 033616 (2005).
[24] M. Sigrist, H. Tsunetsugu, and K. Ueda, Phys. Rev. Lett. **67**, 2211 (1991).
[25] B. M. Peden, D. Meiser, M. L. Chiofalo, and M. J. Holland, Phys. Rev. A **80**, 043803 (2009).
[26] B. Paredes *et al.*, Nature (London) **429**, 277 (2004).